Range-Optimized Theory of Polyelectrolyte Solutions: Basic Theory and Application to Rod Polymers

James P. Donley*

The Boeing Company, Huntington Beach, California 92647

David R. Heine

Sandia National Laboratories, Albuquerque, New Mexico 87185

David T. Wu

Departments of Chemistry and Chemical Engineering, Colorado School of Mines, Golden, Colorado 80401

Received April 15, 2004; Revised Manuscript Received November 4, 2004

ABSTRACT: We present a theory for the equilibrium structure of polyelectrolyte solutions. The main element is a simple and general optimization scheme that allows theories such as the random phase approximation to handle the strong repulsive forces present in such systems. Charged hydrophilic rods in salt-free solution at semidilute densities are examined. The effect of including condensed counterions is analyzed. Comparison with other theories is made. Results of experiments of hydrophilic polyelectrolytes with monovalent counterions in salt-free solution have shown that the structure factor peak position and height can become invariant at high charge fraction. We show that this invariance may be the result of polymer−polymer correlations rather than the conventional explanation involving counterion condensation. On the other hand, as determined by the osmotic pressure, it is found that the solution can become mechanically unstable to macrophase separation at high charge fraction. In this case, adding *explicit* condensed counterions acts to stabilize the liquid, that is, *intra*chain correlations between condensed counterions, not contained in the idealized Manning−Oosawa theory, must be included.

1. Introduction

Polyelectrolytes continue to be of great research interest due to their use in many industrial applications, as well as their presence in biological systems. While polyelectrolytes can have complex architectures and interact with themselves and their surroundings in many different ways, in this work, we focus on their general characteristics. Specifically, this work describes a theoretical study of the liquid structure of long, linear polyelectrolytes in solution.[1] Even for this "simple" system, the properties of polyelectrolytes have proven to be rich, with many unanswered questions even after more than fifty years of study.[2−4]

There have been two basic theoretical approaches to the study of liquid structure in polyelectrolyte solutions. In one, the motion of the polymers is restricted or neglected and the object of interest is the correlations between the counterions and the stationary polymers or between the counterions themselves.[5,6] The mean-field Poisson−Boltzmann (PB) theory[7,8] is commonly employed. It has been successful in predicting the counterion distribution about isolated rods or in periodic cells in comparison with simulations of the same geometry or even experiment.[9−11] However, this agreement is restricted to cases in which the mean-field approximation is valid. The usual rule is that PB theory is less reliable if the density of polymer is high or the system is far above the Manning−Oosawa (M−O) condensation limit, i.e., the Bjerrum length is large or the counterions are multivalent.[8−10] On the other hand, extensions of PB theory that account approximately for steric repulsion between ions and other ion−ion correlations have yielded qualitative agreement with simulation or experiment for charge inversion[9] and counterion layering at surfaces.[12] Also, an extension of the theory to dilute assemblies of randomly ordered rods[13] performs well in comparison with simulation.[14] A variation of this approach is to analyze the forces between two or more rods due to their direct interactions and the surrounding counterion cloud.[6,15−17] In this manner, "counterion-induced attractions" can be examined. This mechanism is usually given as the explanation for the negative osmotic pressures observed in some simulations[11,18] of charged rods that the basic PB theory itself does not capture. The second approach is complementary to the first. Here, correlations between polymers are of first importance. Typically, the free counterions are treated in a Debye−Hückel (D−H) approximation,[19−21] though in some studies, they have been included explicitly.[21−25]

Here, we take the second approach. The main reason for this direction is that most experiments are of isotropic liquids, so this route allows one in principle to make direct comparison with scattering experiments. We restrict our analysis in this work to densities in which the correlations between polymers are expected to be the strongest: the semidilute regime. There already exist theories for liquid structure for these densities.[19−22] However, each has either not been applied to or not been shown to be consistently reliable at large, experimentally relevant, interaction energies and charge densities. For example, consider the Manning parameter, $\xi_M = l_B/b^*$, which is one measure of the strength of interactions in a polyelectrolyte system.[5] Here, l_B is the Bjerrum length, which is the range at which the Coulomb energy equals the thermal energy:

* E-mail address: jdonley@mailaps.org.

10.1021/ma049264m CCC: $30.25
Published on Web 01/04/2005

$e^2/(\epsilon k_B T)$, where e, ϵ, k_B, and T are the electron charge, solvent (usually water) dielectric constant, Boltzmann's constant, and absolute temperature, respectively. The length b^* is the distance between charges along the chain. For typical highly charged polyelectrolytes in water $\xi_M \approx 3$.[26,27] We know of no theory, one that includes explicit counterions and models properly the local correlations in the liquid, that has been shown to have a convergent solution for long chains throughout the semidilute regime at these large values of ξ_M. Theories that model counterions implicitly using, e.g., screened Coulomb interactions between polymer monomers, can give solutions at higher values of the Manning parameter, but the D−H modeling of counterion behavior makes the accuracy of their predictions unknown in the absence of quantitative comparison with simulation, experiment, or more realistic theories.

Our goal here is to create a theory that can be compared quantitatively with experiment at these large Manning parameters. Despite its simple form, the random phase approximation (RPA) can give reasonable predictions for the free energy of polyelectrolyte solutions.[28−30] However, theories such as the RPA fail for structure because they model incorrectly the behavior of the liquid on short and intermediate lengthscales (which translates to a failure on long lengthscales also). Our solution here is to improve the behavior of theories such as the RPA on these lengthscales by generalizing a technique popular in liquid-state theory for short-range interactions to the intermediate-range ones in charged systems. When applied to the RPA, the resultant theory is able to handle the strong polymer−polymer repulsions yet is also able to include the effect the explicit counterions at large interaction energies. Improvements in counterion−polymer correlations are then done by adding condensed counterions (CC's) to the theory using a model such as the popular two-state.[28,29,31] In this manner we can attempt to answer a number of questions that have arisen from experiment yet have not been analyzed by any theory in a quantitative way. Since the RPA theory is used as the base theory, effects that rely on strong three-body or higher correlations such as counterion-induced attractions are not expected to be modeled well. However, if the RPA proves to be insufficient, the optimization technique introduced here can be applied to other theories.

The space of possible polyelectrolyte systems is immense. In the work here, this "range-optimized" (RO) theory is applied to the simplest polyelectrolyte system: uniformly charged rods with hydrophilic backbones and monovalent counterions in a salt-free, continuum dielectric solution. This system is known as the rod "primitive" model of polyelectrolytes. It is well-known that charged rods can order nematically at high density; so, given that most experiments deal with flexible chains, it might seem that including chain flexibility would be a better first test of the theory. However, as chain structure for flexible chains varies greatly with density, charge fraction, etc., including that aspect would cloud the basic predictions of the theory, so it has not been included. Following work of others[32] using the polymer reference interaction site model (PRISM), the theory here could be extended to describe nematic ordering, but the results below will deal only with the isotropic case.

The remainder of this work is organized as follows. In Section 2.1, we discuss the basic field theory approach to the RPA and its higher loop improvements and our method to improve them. In Section 2.2, we discuss how to solve numerically this range-optimized RPA theory. In Section 2.3, we discuss the various models of the polyelectrolyte solution that we will explore, one being the "two-state" that includes the effect of condensed counterions. In Section 2.4, we present our form for the system free energy used to compute the number of condensed counterions per chain in this two-state model. In Section 3, we present results of the RO−RPA theory for the semidilute regime for various models and compare with the RPA and other theories. We find that this RO−RPA theory predicts a number of interesting qualities of the structure factor and radial distribution function. In Section 4, we summarize our results and discuss future work.

2. Theory

2.1. Range Optimization. The system of interest here is a mixture of charged polymers with dissociated counterions in polar solvent. However, for generality, consider a liquid of different types of molecules in a volume V at temperature T. Let all molecules be composed of spherical sites, and let N_M be the number of molecules of type M and N_{Mk} denote the number of sites of type k on a molecule of type M. Then, the average molecule and site number densities are $\rho_M = N_M/V$ and $\rho_{Mk} = N_M N_{Mk}/V$, respectively. Let all sites possibly be charged with Z_{Mk}, denoting the valency (0, ±1, ...) of a site of type k on a molecule of type M. All interactions are assumed to be pairwise decomposable; so, let $u_{MkM'k'}(r)$ be the potential between a site of type k on the molecule of type M and a site of type k' on a molecule of type M' a distance $r \equiv |\mathbf{r}|$ apart. For present purposes, $u_{MkM'k'}(r)$ is infinite for $r < \sigma_{MkM'k'}$, $\sigma_{MkM'k'}$ being the hard-core diameter between the two sites. For $r > \sigma_{MkM'k'}$, the potential has a long-ranged tail, $u_{MkM'k'}(r) = u^{\mathrm{lr}}_{MkM'k'}(r)$. Depending on the model, this long-ranged tail has either a Coulombic or screened Coulomb form. It can also contain a shorter ranged component to mimic a van der Waals interaction or hydrogen bonding. In what follows, all interactions are scaled in units of the thermal energy, $k_B T$.

In this work, we focus on understanding mainly the density correlations in a polyelectrolyte solution in equilibrium. Most experiments probe these correlations using scattering techniques. To this end, let $I(q)$ be the intensity of scattered radiation (light, X-ray, neutrons, etc.) at momentum transfer q. We restrict ourselves here to static scattering experiments so $I(q)$ is independent of time. In the single scattering limit, i.e., Born approximation, $I(q)$ is proportional to the weighted sum of the partial structure factors $S_{MkM'k'}(q)$. The inverse Fourier transform of the structure factor is the density−density correlation function and relates theory to experiment. It is defined by

$$S_{MkM'k'}(r) = \langle(\hat{\rho}_{Mk}(\mathbf{r}) - \rho_{Mk})(\hat{\rho}_{M'k'}(0) - \rho_{M'k'})\rangle \tag{1}$$

where

$$\hat{\rho}_{Mk}(\mathbf{r}) = \sum_{i,\alpha} \delta(\mathbf{r} - \mathbf{r}_{Mik\alpha}) \tag{2}$$

is the microscopic density of sites of type k on molecules of type M at position $\mathbf{r}$, with $\mathbf{r}_{Mik\alpha}$ being the position of the αth site of type k on the ith molecule of type M. The brackets denote a thermodynamic average, and $\delta(\mathbf{r})$ is the Dirac "delta" function. This correlation function can be separated into *intra*- and *inter*molecular pieces, $\Omega_{MkM'k'}(r)$ and $H_{MkM'k'}(r)$, respectively:

$$S_{\mathrm{MkM'k'}}(r) = \Omega_{MkM'k'}(r) + H_{\mathrm{MkM'k'}}(r) \tag{3}$$

The intramolecular structure function is defined by

$$\Omega_{MkM'k'}(r) = \rho_M \delta_{MM'} \sum_{\alpha,\beta} \langle \delta(\mathbf{r} - \mathbf{r}_{M1k\alpha} + \mathbf{r}_{M1k'\beta}) \rangle \qquad (4)$$

where $\delta_{MM'}$ is the Kronecker delta. This function can be computed either a priori if the molecular architecture is known, as for rod polymers (see below), or self-consistently along with intermolecular correlation functions such as $H_{MkM'k'}(r)$, as for flexible polymers.[19,33−35] The total intermolecular correlation function $H_{MkM'k'}(r) = \rho_{Mk}\rho_{M'k'}[g_{MkM'k'}(r) - 1]$, where $g_{MkM'k'}(r)$ is the radial distribution function defined by

$$g_{MkM'k'}(r) = \frac{1}{N_{Mk}N_{M'k'}} \sum_{\alpha,\beta} \langle V\delta(\mathbf{r} - \mathbf{r}_{M1k\alpha} + \mathbf{r}_{M'2k'\beta}) \rangle \qquad (5)$$

To compute these intermolecular correlations it is helpful to define a function

$$\Delta_{MkM'k'}(r) \equiv \langle \phi_{Mk}(\mathbf{r}) \phi_{M'k'}(0) \rangle \qquad (6)$$

where the field $\phi_{Mk}(\mathbf{r})$ is conjugate to $\hat{\rho}_{Mk}(\mathbf{r})$, as defined by the Hubbard−Stratonovich transformation (i.e., generalized Gaussian integral).[36] A well-known, simple, and exact relation between Δ and S is[37]

$$S_{MkM'k'}(r) = u^{-1}_{MkM'k'}(r) - \sum_{NlN'l'} u^{-1}_{MkNl} * \Delta_{NlN'l'} * u^{-1}_{N'l'M'k'}(r) \qquad (7)$$

where the asterisks (*) denote convolutions

$$A * B(\mathbf{r}) \equiv \int d\mathbf{r}' A(\mathbf{r} - \mathbf{r}') B(\mathbf{r}') \qquad (8)$$

and the quantity $u^{-1}_{MkM'k'}(r)$ is the functional inverse of $u_{\mathrm{MkM'k'}}(r)$ defined by

$$\sum_{Nl} \int d\mathbf{r}' u_{MkNl}(\mathbf{r} - \mathbf{r}') u^{-1}_{NlM'k'}(\mathbf{r}' - \mathbf{r}'') = \delta_{MM'}\delta_{kk'}\delta(\mathbf{r} - \mathbf{r}'') \qquad (9)$$

In terms of the potentials, u, and molecular structures, the effective interaction, Δ, has the form

$$\Delta^{-1}_{MkM'k'}(r) = u^{-1}_{MkM'k'}(r) + \Omega_{MkM'k'}(r) + \zeta_{MkM'k'}(r) \qquad (10)$$

where $\zeta_{MkM'k'}(r)$ contains all terms beyond one-loop order. If one lets $\zeta_{MkM'k'}(r) = 0$, then combining eqs 3, 7, and 10 yields the familiar RPA equation for $H_{MkM'k'}(r)$. The advantage of the RPA expression is that it is simple to solve yet produces an important property of real liquids: screening. The disadvantage of the RPA is that it does not work well for structure if the interactions are strong. For example, the RPA predicts for rod polymers that the first nonzero peak wavevector, $q_{\max}$, in the monomer−monomer structure factor $S_{\mathrm{pmpm}}(q) \equiv S_{\mathrm{mm}}(q)$ scales with density ρ_{m} in the semidilute regime as ρ_{m}^{ν} with exponent $\nu = 1/3$. On the other hand, experiment and simulation have shown that $\nu \approx 1/2$, which is also the value for dense hard-core molecules.[3] It is thought that the cause of this deficiency and others is that the RPA does not model well the short and intermediate lengthscale density correlations, in particular the large repulsion between like-charged molecules. This deficiency in turn causes the long-range correlations to also be incorrect. One remedy is to compute the higher-order terms embodied in $\zeta_{MkM'k'}(r)$ in some approximate manner, usually by partial diagram summation. There have been some successes with this approach.[19] However, the need to handle the strong interactions, polymer nature, and other effects all at once makes this path a difficult one.

There have been other attempts to correct these short and intermediate lengthscale deficiencies (and almost all of these are in the context of computing the free energy to obtain thermodynamics). An interesting method due to Ermoshkin and Olvera de la Cruz is to introduce a density-dependent cutoff into the field theory.[30] This cutoff enables the theory to overcome the breakdown of the RPA on lengthscales shorter than the correlation length and attain qualitative agreement with the predictions of Jiang et al.[38] for the phase behavior of polyelectrolytes. However, by neglecting fluctuations on lengthscales smaller than, e.g., the correlation length, the coupling of these fluctuations to longer-wavelength ones is also neglected. While it appears that such coupling may be less important for thermodynamics, it is very important for liquid structure. Another method is to apply the "EXP" approximation of Andersen and Chandler[39] to polyelectrolytes.[38] While this method does enforce the positivity of the radial distribution function, it neglects the coupling of this change in $g(r)$ at short lengthscales to longer-wavelength ones so that, for example, the density dependence of the correlation length is no different than for the RPA. As a consequence, we take an alternative path and ask the question: Is it possible to make the RPA adequate for describing density correlations given a suitable reinterpretation of the interaction potentials?[40] The goal here is not necessarily to capture three-body effects such as counterion-induced attractions or even condensation (though including such effects would surely be welcome) but just the ordering and screening in the liquid.

The failure of the RPA to model well the large repulsions between like-charged molecules is manifested in a large negative radial-distribution function $g(r)$ for short distances even though that function is intrinsically nonnegative. For short-range repulsive, e.g., hard-core, potentials, one remedy to this deficiency in the radial distribution functions was proposed by Andersen and Chandler (AC).[40] Their idea was to replace the true potential, u, by an optimized one, $\tilde{u}_{MkM'k'}(r)$. For distances $r < \sigma_{MkM'k'}$, $\tilde{u}_{MkM'k'}(r)$ takes a value such that the hard-core condition is satisfied, i.e., $g_{MkM'k'}(r) = 0$. Outside the core, $\tilde{u}_{MkM'k'}(r)$ can be set equal to the original potential, $u(r)$, which is long-ranged and presumably weak. In this way, higher-order diagrams neglected in the theory are summed in an approximate manner to enforce the core condition. When applied to the RPA, this optimization scheme is a generalization of the Mean Spherical Approximation (MSA) closure[41] to the Ornstein−Zernike (OZ) equation,[42] and a closely related scheme has been shown to be diagrammatically proper[43,44] for one generalization of OZ to molecules, the theory of Chandler, Silbey, and Ladanyi (CSL).[45] This optimized RPA or ORPA, usually with long-range potentials absent, is more popularly known as RISM for small molecules[46] and PRISM for polymers.[47]

Unfortunately this Andersen−Chandler optimization is not very useful for polyelectrolytes. One reason is that the contact energy between ion and counterion seems to be less important than the interaction energy of the counterion with the whole chain. Hence, enforcing the hard-core behavior between opposite charges matters less than modeling correctly the chain structure, e.g., determining the bond length, b. A more important reason is that the repulsion between like-charged polymers is usually very large. This causes the radial distribution function to be effectively zero out to a distance that appears to scale with density in the semidilute regime in the same manner as the D−H screening length. For highly charged chains, this distance is usually much larger than the hard-core size.[20−22,48] Hence, enforcing the core condition produces little improvement in the theory for long polyelectrolytes.

Here, we propose an alternative scheme: we optimize the *range* of the pseudo-hard-core portion of $\tilde{u}(r)$, and not just its amplitude. By this we mean that if $g(r)$ is nearly zero out to some distance, then it makes little difference whether this exclusion zone is caused by a hard-core potential or a Coulombic one. This effective hard-core diameter $\sigma^{\mathrm{eff}}_{MkM'k'}$ is determined by requiring that $g_{MkM'k'}(r)$ be nonnegative everywhere (not just zero inside the core). The closure to the theory then is

$$g_{MkM'k'}(r) = 0, \quad r < \sigma^{\text{eff}}_{MkM'k'}$$
$$\tilde{u}_{MkM'k'}(r) = u_{MkM'k'}(r), \quad r > \sigma^{\text{eff}}_{MkM'k'} \tag{11}$$

and the range $\sigma^{\text{eff}}_{MkM'k'}$ of the hard-core interaction is chosen to have the smallest value such that $g_{MkM'k'}(r) > 0$ for $r > \sigma^{\text{eff}}_{MkM'k'}$ subject to the constraint that $\sigma^{\text{eff}}_{MkM'k'} \geq \sigma_{MkM'k'}$.

While eq 11 is a general relation, the simplest way to explore its consequences is to apply it to the most basic theory appropriate for molecular liquids, the RPA. The rest of this work will focus on that application. We shall refer to this theory as range-optimized RPA, denoted as RO-RPA. With known forms for $\Omega_{MkM'k'}(q)$ and the potential $u_{MkM'k'}(r)$, as well as setting $\zeta_{MkM'k'}(r) = 0$, eqs 3, 7, 10, and 11 form the closed set of equations for the RO-RPA theory.

2.2. Numerical Solution. In this section, we discuss how the RO-RPA theory is solved numerically. The method is very similar to the standard Picard type used in atomic Ornstein−Zernike theory or molecular or polymer RISM-type theories.[47,49]

Given the mixed closure, eq 11, it is necessary to solve for $h_{MkM'k'}(r) \equiv g_{MkM'k'}(r) - 1$ and $\tilde{u}_{MkM'k'}(r)$ simultaneously. In RO-RPA, as in RISM or PRISM, all integrals are convolutions and reduce to products in reciprocal space, and so are solved using Fourier transform methods. However, the difficulty of solving for correlation functions for a polyelectrolyte system over the more-common van der Waals ones is that the long-range Coulomb interaction requires that the system size, $r_{\max}$, be effectively infinite to perform any Fourier transform. One way to deal with Coulomb systems while keeping $r_{\max}$ of moderate value is due to Hoye, Lomba, and Stell.[20,50] The basic idea is to solve *exactly* for the theory in the large r limit and then subtract that behavior, yielding a theory in which the functions rapidly go to zero as $r \to \infty$ (at least away from the critical point). The description below applies to systems in which the molecules interact through full Coulomb potentials, but it can be trivially modified to also handle others as well. The Coulomb potential $u^{\text{coul}}_{MkM'k'}(r)$ has the well-known form:

$$u^{\text{coul}}_{MkM'k'}(r) = \frac{Z_{Mk}Z_{M'k'}l_{\text{B}}}{r} \tag{12}$$

First, using eqs 3, 7, 10, and 12, it can be shown easily that since $\tilde{u}_{MkM'k'}(r) \to u^{\text{coul}}_{MkM'k'}(r)$ as $r \to \infty$, then $h_{MkM'k'}(r) \to h^{\text{rpa}}_{MkM'k'}(r)$, the RPA solution for $h_{MkM'k'}(r)$. Thus, $\tilde{u}_{MkM'k'}(r)$ and $h_{MkM'k'}(r)$ can be split into short- and long-range pieces,

$$\tilde{u}_{MkM'k'}(r) = \tilde{u}^{\text{sr}}_{MkM'k'}(r) + u^{\text{rpa}}_{MkM'k'}(r)$$
$$h_{MkM'k'}(r) = h^{\text{sr}}_{MkM'k'}(r) + h^{\text{rpa}}_{MkM'k'}(r) \tag{13}$$

Here, "rpa" denotes the RPA solutions of these functions with $\tilde{u}_{MkM'k'}(r)$ set to $u^{\text{rpa}}_{MkM'k'}(r) \equiv u^{\text{coul}}_{MkM'k'}(r)$ for all r. For an atomic Coulombic system, the RPA solution for $h^{\text{rpa}}_{MkM'k'}(r)$ and its Fourier transform, $h^{\text{rpa}}_{MkM'k'}(q)$, can be solved exactly analytically. These exact solutions can be used then to obtain numerically the molecular form for $h^{\text{rpa}}_{MkM'k'}(r)$ and its Fourier transform.[21] The functions $\tilde{u}^{\text{sr}}$ and h^{sr} are short ranged and so can be Fourier transformed in the usual manner. With these equations, the resultant theory is solved as follows. An initial guess is obtained for all the effective hard-core diameters, $\sigma^{\text{eff}}_{MkM'k'}$. Then, with an initial guess for $\tilde{u}_{MkM'k'}(q)$ and the previously obtained $u^{\text{rpa}}_{MkM'k'}(q)$, the function $h_{MkM'k'}(r)$ is determined using the RPA equation, making sure to subtract $h^{\text{rpa}}_{MkM'k'}(q)$ before inverse Fourier transforming and then adding back $h^{\text{rpa}}_{MkM'k'}(r)$ afterward. With $h_{MkM'k'}(r)$, a new function $g^{<}_{MkM'k'}(r)$ is defined. This function equals $g_{MkMk'k'}(r)$ inside the core, $r < \sigma^{\text{eff}}_{MkM'k'}$, but is set to zero outside. A new function is defined

$$\gamma_{MkM'k'}(r) = \rho_{Mk}\rho_{M'k'}\sum_{NlN'l'}\Omega^{-1}_{MkNl} * g^{<}_{NlN'l'} * \Omega^{-1}_{N'l'M'k'}(r) + \tilde{u}_{MkM'k'}(r) \tag{14}$$

Upon convergence, $g^{<}(r)$ vanishes but is added to accelerate convergence without changing the final result. With $\gamma_{MkM'k'}(r)$, the closure, eq 11, above can be used to obtain new values for $\tilde{u}^{\text{sr}}$:

$$\tilde{u}^{\text{sr}}_{MkM'k'}(r) = \begin{cases} \gamma_{MkM'k'}(r), & r < \sigma^{\text{eff}}_{MkM'k'} \\ \tilde{u}^{\text{lr}}_{MkM'k'}(r) - \tilde{u}^{\text{rpa}}_{MkM'k'}(r), & r > \sigma^{\text{eff}}_{MkM'k'} \end{cases} \tag{15}$$

Note that $u^{\text{lr}}(r)$ is not necessarily equal to $u^{\text{rpa}}(r) \equiv u^{\text{coul}}(r)$ if other short-range interactions such as van der Waals are included. The solutions are then mixed, typically at an old-to-new ratio of 99:1 and Fourier transformed to obtain the new $\tilde{u}^{\text{sr}}_{MkM'k'}(q)$. The equations are iterated until convergence is obtained. With this new solution, it is determined whether each component $g_{MkM'k'}(r) > 0$ for all r. If it is not, then $\sigma^{\text{eff}}_{MkM'k'}$ is increased. If it is and if $\sigma^{\text{eff}}_{MkM'k'} > \sigma_{MkM'k'}$, then it is determined if $g_{MkM'k'}(r)$ is approximately zero at $r = \sigma^{\text{eff}}_{MkM'k'}$. If it is larger than some amount, e.g., 10^{-3}, then $\sigma^{\text{eff}}_{MkM'k'}$ is reduced. Given these new values, the above algorithm is solved again for $g_{MkM'k'}(r)$. Depending on the initial guess, it takes typically two to eight iterations on the effective hard-core diameters to achieve convergence.

The functions were solved on a grid of N_{latt} points for $0 < r \leq r_{\max}$ with a spacing Δr (or $\Delta q = \pi/(N_{\text{latt}}\Delta r)$ in reciprocal space). The number of points and grid spacing typically vary with density.

Last, all computations were performed on an Athlon PC running under either RedHat Linux 7.3 or SuSE Linux 9.0.

2.3. Polyelectrolyte Models. We will consider in this work four models of polyelectrolytes in solution. There will be three types of sites for these models: polymer ion monomers, free counterions, and counterions confined to the surface of the polymer backbone. To fix notation, let "c" and "m" denote counterions and polymer monomers, respectively. Also, let "p" and "f" denote the polymer and counterion molecules, respectively. For example, "fc" denotes a free counterion site.

As stated above, we confine our analysis to charged rod polymers and their associated counterions in salt-free solution. The monomers and counterions are monovalent, and the polymer backbone is taken to be intrinsically hydrophilic. We further assume that the polyelectrolytes are "strong". By this term, we mean that all monomers that have dissociated remain so under all conditions. The charges then are quenched as opposed to annealed. We also assume that effects of the solvent can be well captured by a single quantity, the dielectric constant, ϵ, that appears in the Bjerrum length, l_{B}, defined above. We then ignore possible effects such as the solvent surrounding the polymer and counterions and shielding them from each other. That is, we assume that the local structure of the liquid does not matter much for the phenomena that we shall explore. We then need not be too precise in modeling the local chain architecture or even the monomer sizes. To that end, we let all monomers and counterions be of equal size, so $\sigma_{MkM'k'} = \sigma$ for all $MkM'k'$. For simplicity, we also let the polymer bond length $b = \sigma$. Since the polymers are intrinsically hydrophilic polymers, we can ignore any other interactions except Coulomb (or screened Coulomb) in $u^{\text{lr}}_{MkM'k'}(r)$. Most synthetic polyelectrolytes are randomly charged.[26,27] We model this randomness of the polymer charge by letting our model polymer be uniformly charged, but allowing the monomer charge, $Z_{\text{pm}} \equiv Z_{\text{m}}$, to vary continuously: $0 \leq Z_{\text{m}} \leq 1$, so $Z_{\text{m}} \equiv f$, the per chain average fraction of charged monomers. We set $Z_{\text{pc}} = Z_{\text{fc}} \equiv Z_{\text{c}} = -1$. With a known monomer density $\rho_{\text{pm}} \equiv \rho_{\text{m}}$, the total counterion density $\rho_{\text{c}} \equiv \rho_{\text{pc}} + \rho_{\text{fc}}$ is determined by charge neutrality: $\Sigma_{Mk}Z_{Mk}\rho_{Mk} = 0$.

With the restrictions or assumptions above, it is of interest to then examine predictions of models with varying degrees of realism. Here, we consider four models of polyelectrolytes in solution: the minimal, primitive, two-state implicit, and

two-state explicit. In the minimal model, the system consists of a gas of charged rods with sites that interact via a screened Coulomb potential, so $u^{\rm lr}_{\rm mm}(r) = u^{\rm sc}_{\rm mm}(r)$, where

$$u^{\rm sc}_{\rm mm}(r) = \frac{Z_{\rm m}{}^2 l_{\rm B}}{r}\exp(-\kappa r) \tag{16}$$

and the inverse D−H screening length $\kappa = \sqrt{4\pi l B Z_c{}^2 \rho_c}$ is due to the counterions. In the primitive model (used in analogy with the primitive model of electrolyte theory), the system consists of a gas of uniformly charged polymers (rods here) and counterions with sites that interact via a full Coulomb potential, so $u^{\rm lr}_{MkM'k'}(r) = u^{\rm coul}_{MkM'k'}(r)$, given by eq 12 above.

As will be seen below, the range optimization technique allows one to modify a theory so that the large repulsions are handled properly; however, it appears to improve ion−counterion correlations only moderately. When applied to, for example, the RPA, the resultant theory still underestimates correlations between oppositely charged sites. As a consequence, it will be interesting to explore the effects of improving monomer−counterion correlations by some means. The simplest way to do this is to use the popular two-state model.[28,29,31] In this model, the counterions are divided into two species, "free" and "condensed". Free ones are treated as in the primitive model. Condensed ones are bound to the chain. Each chain has the same number of CC's, $N_{\rm pc}$. The average number of CC's is determined by constructing a free energy for the system and then minimizing it with respect to $N_{\rm pc}$. To determine the free energy, we make the standard assumption that the above model of condensed counterions provides a better estimate of counterion behavior near the chain than the original theory.[28,29] If so, then by minimizing the free energy with respect to $N_{\rm pc}$, one obtains improved polymer−counterion correlations by obtaining a better estimate for the free energy. The region of motion of the counterions is split so that the "free" ones are excluded from sampling the CC states and vice versa.[28] In this manner, $N_{\rm pc}$ will always be nonzero, but for the densities that we consider here, $N_{\rm pc}$ will be negligible until the system approaches the idealized M−O condensation threshold. Here, we treat the CC's in two ways, implicitly and explicitly. In the first, the system is the same as the primitive, but the monomer charge, $Z_{\rm pm}$, is reduced to account for the CC's: $Z_{\rm pm} \rightarrow Z_{\rm pm} + N_{\rm pc}/N_{\rm pm}Z_{\rm pc}$, where $N_{\rm pm}$ is the number of backbone monomers per chain. The idea behind this approximation is the common one that the main purpose of CC's is to reduce the effective charge on the chain. In the second, the CC's are treated as an additional type of site on the chain with interactions that are the same as in the primitive model. In this explicit model, the CC's are confined to the surface of the chain but are allowed to freely translate along its length. Let the polymer backbone be along the Z axis with an end site at $Z = 0$. Allowed CC states were then at $Z = 0$, b, $2b$, ..., $(N_{\rm pm} - 1)b$, with a radial distance $r = \sigma$ and possible azimuthal angles $\phi = 0$, $\pi/2$, π, and $3\pi/2$. Having only discrete states was done for computational efficiency; other ways to model the surface floating of the CC's changed $N_{\rm pc}$ by a few percent at most as long as $N_{\rm pc}/N_{\rm pm} \leq 1/2$. The main difference between the implicit and explicit models is that the latter allows for *intra*molecular correlations between CC's. As we will see below, the differences between these two models can be large.

2.4. Intramolecular Correlation Functions and Free Energy. The theory above is completed by specifying the intramolecular correlation functions and, for the two-state model, the number, $N_{\rm pc}$, of CC's per chain. The latter requires an evaluation of the system free energy.

Since the chain backbone is a rod, the Fourier transform of the monomer−monomer intramolecular correlation function, eq 3, has the well-known form:

$$\Omega_{\rm pmpm}(q) = \rho_{\rm pm}\left[1 + \frac{2}{N_{\rm pm}}\sum_{\alpha=1}^{N_{\rm pm}-1}(N_{\rm pm} - \alpha)\sin(\alpha q b)/(\alpha q b)\right] \tag{17}$$

If the CC's are implicit, then knowing $\Omega_{\rm pmpm}(q)$ is sufficient. For that model, one then just reduces the monomer charge $Z_{\rm pm}$ to $Z_{\rm pm} + N_{\rm pc}/N_{\rm pm}Z_{\rm pc}$ to account for the CC's. For the explicit model, the CC's are a separate type of site and so $\Omega_{\rm pmpc}(q)$ and $\Omega_{\rm pcpc}(q)$ must be also computed. The simplest way to compute the chain statistics is to use the very popular concept of an effective single-chain Hamiltonian, $\mathscr{H}^{\rm eff}_{\rm M}\{\mathbf{r_M}\}$, where $\{\mathbf{r_M}\}$ denotes a particular configuration of the chain.[51] It has the form

$$\mathscr{H}_{\rm M}{}^{\rm eff}\{\mathbf{r_M}\} = \mathscr{H}_{\rm 0M}\{\mathbf{r_M}\} + \sum_{kk'}\sum_{\alpha\beta} u^{eff}_{MkMk'}(\mathbf{r}_{M1k\alpha} - \mathbf{r}_{M1k'\beta})(1 - \delta_{kk'}\delta_{\alpha\beta}) \tag{18}$$

where $\mathscr{H}_{\rm 0M}\{\mathbf{r_M}\}$ is the "bare" Hamiltonian for a molecule of type M in a configuration $\{\mathbf{r_M}\}$. It contains bonding potentials and other constraints. As discussed in Section 2.3 above, the CC's are constrained to lie on the surface of the chain backbone but are free to translate up and down it, and so $\mathscr{H}_{\rm 0M}$ contains such information. The function $u^{\rm eff}_{MkMk'}(r)$ is an effective potential between sites of type k and k' on a molecule of type M. It contains the direct potential $u_{MkMk'}(r)$ (ignoring those terms already in $\mathscr{H}_{\rm 0M}$) and a medium-induced potential $u^{\rm mip}_{MkMk'}(r)$ that mimics the effects (mostly screening) of the other molecules in the liquid. This medium-induced potential thus depends on intermolecular correlation functions such as $g_{MkM'k'}(r)$, and so normally they and the Ω's would be computed in a self-consistent manner. However, for rods for the cases considered in this work, it proved sufficient to just let $u^{\rm eff}_{MkMk'}(r)$ have a screened Coulomb form outside the core. That is, we let

$$u^{\rm eff}_{MkMk'}(r) = \begin{cases} \infty, & r < \sigma_{MkMk'} \\ \dfrac{Z_{Mk}Z_{Mk'}l_B}{r}\exp(-\kappa_t r), & r > \sigma_{MkMk'} \end{cases} \tag{19}$$

where the inverse screening length $\kappa_t = \sqrt{4\pi l_{\rm B}[\rho_m Z^2_{\rm m} + \rho_c Z^2_{\rm c}]}$ is due to both ions and counterions. Given eqs 18 and 19, it is straightforward to compute the intramolecular structure functions by Monte Carlo simulation.

The second element needed for the two-state model is an expression for the total system Helmholtz free energy, $F_{\rm tot}$. For this system, $F_{\rm tot}$ is a function of V, T, and $N_{\rm p}$(or $N_{\rm pm}$), so it can be written as $Vf(T,\rho_p)$ where f is the free energy density. The number of counterions is fixed by charge neutrality and so is not an independent variable. Minimization of this free energy with respect to $N_{\rm pc}$ will yield the average number of CC's per chain and thus complete the theory. Since we have chosen to demonstrate the consequences of our range optimization approach using the RPA theory, one might think that using the RPA expression for $F_{\rm tot}$ with $u(r) \rightarrow \tilde{u}(r)$ would give an accurate value for $N_{\rm pc}$. However, if this form is used, we find that $N_{\rm pc} = 0$ for RO-RPA for cases with realistic temperatures and bond lengths. So instead, we employ the charging method to compute $F_{\rm tot}$.

In the charging method, $F_{\rm tot}$ can be represented as a sum of contributions,

$$F_{\rm tot} = F_{\rm id} + F_{\rm hc} + F_{\rm lr} \tag{20}$$

First, $F_{\rm id}$ is the free energy with all hard-core and long-range interactions turned off. We find,

$$F_{\rm id}/V = \rho_{\rm p}\log(\rho_{\rm p}\sigma^3) + \rho_{\rm f}\log\left(\frac{\rho_{\rm f}\sigma^3}{1 - \rho_{\rm p}N_{\rm pm}\tilde{v}}\right) - \rho_{\rm p}\log(\tilde{Z}_0) + \{\text{irrelevant terms}\} \tag{21}$$

where ρ_p and ρ_f are the polymer and free counterion molecular densities, respectively, and $N_{pm}\tilde{v}$ is the region of motion of a CC. Since the monomers and counterions are the same size and mass, in eq 21 we have set both their thermal wavelengths equal to the hard-core diameter, σ, for convenience. Here, $\tilde{Z}_0$ is the reduced partition function for a single molecule with all nonbonding potentials turned off. For rods, we count only the entropy of CC's and so let[28,29]

$$\log(\tilde{Z}_0) \approx N_{pc}\log\left(\frac{N_{pm}\tilde{v}}{N_{pc}\sigma^3}\right) \tag{22}$$

In the above CC model, the CC's are confined to the chain surface. Hence, the region of motion excluded from the free counterions is just the chain backbone volume. So, $\tilde{v}/\sigma^3 \approx 1$.

The term F_{hc} is the contribution to F_{tot} from turning on the hard-core interactions from the ideal state. It has the usual form:[52]

$$F_{hc}/V = \frac{2\pi}{3}\sum_{MM'}\sum_{kk'}(\sigma_{MkM'k'})^3\int_0^1 dx\ \rho_{Mk}\rho_{M'k}g^{(0)}_{MkM'k'}(x^{1/3}\sigma_{MkM'k'}+, x) \tag{23}$$

Here $g^{(0)}_{MkM'k'}(r, x)$ is the radial distribution for a hard-core system with a hard-core interaction range of $x^{1/3}\sigma_{MkM'k'}$. Letting $r = x^{1/3}\sigma_{MkM'k'}+$ means that the function is evaluated at contact. This hard-core term contributes less than a few percent to the value of F_{tot} at high charge fraction at the densities we consider in this work but is retained for completeness. We ignore the intramolecular hard-core contribution to the free energy.

Last, F_{lr} is the contribution to the free energy from turning on the long-range (e.g., Coulomb) interactions with the hard-core interactions already on. One can easily show that

$$F_{lr}/V = \frac{1}{2}\sum_{MM'}\sum_{kk'}\int d\mathbf{r}\ u^{lr}_{MkM'k'}(r)\int_0^1 d\lambda[\rho_{Mk}\rho_{M'k}g_{MkM'k'}(r,\lambda) + \Omega'_{MkM'k'}(r,\lambda)] \tag{24}$$

Here, $g_{MkM'k'}(r,\lambda)$ and $\Omega'_{MkM'k'}(r,\lambda)$ are the radial distribution function and intramolecular structure function for a system with full hard-core but partial strength long-range interactions $\lambda u^{lr}_{MkM'k'}(r)$. The accent on $\Omega(r)$ indicates that the self-scattering term has been removed. Since the intramolecular structure functions are computed by Monte Carlo simulation, it is a tedious process to compute $\Omega'_{MkM'k'}(r,\lambda)$ for each point in the integral over λ. Instead, we compute all charging integrals, including those in F_{hc}, by assuming that $\Omega'_{MkM'k'}(r,\lambda) \approx \Omega'_{MkM'k'}(r,1)$, i.e., its value at full strength. This additional assumption does not matter for the implicit model (or the minimal or primitive) since N_{pc} is constant during the charging anyways, and so our expression for F_{tot} is essentially exact for that model. For the two-state explicit model, it is approximate since the monomer−CC and CC−CC correlations change as the interactions do, even though N_{pc} is constant. However, our aim here is not a value for the free energy, but only for the position of its minimum with respect to N_{pc}. So, while this approximation will cause N_{pc} to be overestimated, we do not regard that overestimation to be too severe.

To compute the average N_{pc}, we first set it to some value and then compute the full strength chain structure functions Ω's via a Monte Carlo simulation. The charging integrals F_{hc} and F_{lr} are then computed. The PRISM and RO-RPA theories are then used to compute the hard-core and full $g(r)$'s, respectively, according to the algorithm in Section 2.2 above. Now F_{tot} is known. We then increment N_{pc} and repeat the above procedure until the minimum of F_{tot} is determined.

3. Predictions of the RO-RPA Theory

As stated above, our system consists of a solution of uniformly charged rod polymers and their completely dissociated counterions in a salt-free, dielectric continuum. A common polymer used in experiments is a copolymer of acrylamide with sulfonated comonomers which has a bond length $b \approx 2.5$ Å.[27] The Bjerrum length for water at room temperature is $l_B \approx 7.1$ Å. We thus let $l_B/b = 2.85$ for all results below. For reasons discussed in Section 2.3 above, we set $b = \sigma$, $Z_c = -1$, and let $Z_m \equiv f$ vary continuously from 0 to 1. We let $N_{pm} = 400$ in all results below. With this monomer number, the chain overlap density $\rho^*\sigma^3 \approx 10^{-5}$ and is small enough to give a large semidilute regime. The grid spacing, Δr, and number of grid points, N_r, vary with monomer density. For example, for $\rho_m\sigma^3 = 3\times10^{-2}$ and 3×10^{-5} we used $\Delta r = 0.025$, $N_r = 2^{14}$ and $\Delta r = 0.2$, $N_r = 2,^{15}$ respectively. One reason for this variation is that the effective interaction range at large f in the semidilute regime appears to scale with density in the same manner as the D−H screening length, i.e., as $\rho_m^{-1/2}$. Another reason is that the grid spacing determines the precision that one can determine the effective hard-core diameters, $\sigma^{eff}_{MkMk'}$. This graininess matters less for computing correlation functions but more for computing the free energy F_{tot}, eq 20, used to calculate the number of CC's.

To determine the average number of CC's in the two-state models, the charging integrals in F_{hc} and F_{lr}, given in eqs 23 and 24, were computed using the trapezoidal rule with $n_{\lambda hc}$ and $n_{\lambda lr}$ points, respectively. For all the results shown in this work, we set $n_{\lambda hc} = 1$ and $n_{\lambda lr} = 10$, except for greater accuracy at large charge fraction, f, we sometimes set $n_{\lambda hc} = 5$ and $n_{\lambda lr} = 20$.

In the results shown below, by "RPA" theory, we mean that the RPA equation for $g(r)$ is used and the potential $u_{MkM'k'}(r)$ is set to the Coulomb potential $u^{coul}_{MkM'k'}(r)$ for $r > \sigma$ and zero for $r < \sigma$. Setting the potential to zero inside the core rather than letting $u_{MkM'k'}(r) = u^{coul}_{MkM'k'}(r)$ for all r or employing, e.g, the optimized RPA approximation, seems to matter only for very high densities or small charge fractions, f, that is, when the hard-core nature of the polymers becomes important. Hence, while this definition of the RPA theory should be kept in mind when interpreting the results below, the precise approximation to handle the potential inside the core actually does not matter much for the phenomena in which we are interested.

3.1. Radial Distribution Functions. First, we examine how range optimization changes the behavior of the radial distribution functions $g_{MkM'k'}(r)$. Figures 1 and 2 show various $g(r)$'s predicted by the RPA and RO-RPA theories, respectively, within the primitive model. Here, $\rho_m\sigma^3 = 3\times10^{-3}$ and $Z_m = f = 1$. For this density, the D−H screening length due to counterions $\xi = (4\pi l_B Z_c^2\rho_c)^{-1/2} \approx 3\sigma$. The meaning of the curves is shown in the figure legends. As can be seen in Figure 1, the RPA gives strongly negative pmpm ≡ mm correlations for $r < 6\sigma \approx 2\xi$. The fcfc correlations are also slightly negative near contact. The RPA then poorly models the correlation hole effect, as is well known. Now, as can be seen in Figure 2, if one uses the range optimization prescription given in Sections 2.1 and 2.2 above, one finds that the pmpm and fcfc correlations are indeed improved, as the positivity of $g(r)$ is now obeyed. It can also be seen in Figure 2 that the range optimization also increases somewhat the pmfc correlations. While this increased enrichment of counterions near the chain is less than one would expect from an exact theory, it does show that even correlations between attractive sites can be improved by RO. At high charge fraction, we find that

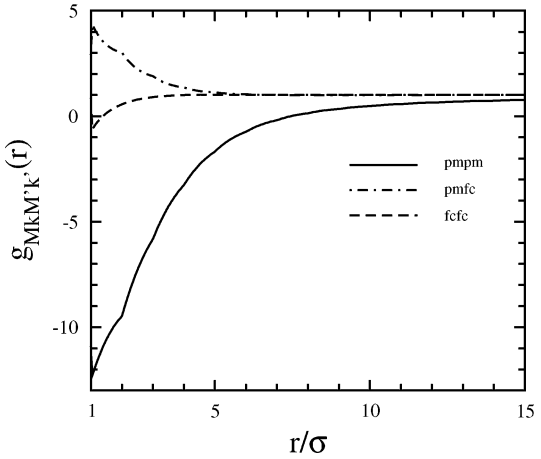

Figure 1. RPA primitive model predictions for the partial radial distribution functions $g_{MkM'k'}(r)$ as a function of scaled distance r/σ. Here, $\rho_m\sigma^3 = 3 \times 10^{-3}$ and $Z_m \equiv f = 1$. The meaning of the curves is shown in the figure legend.

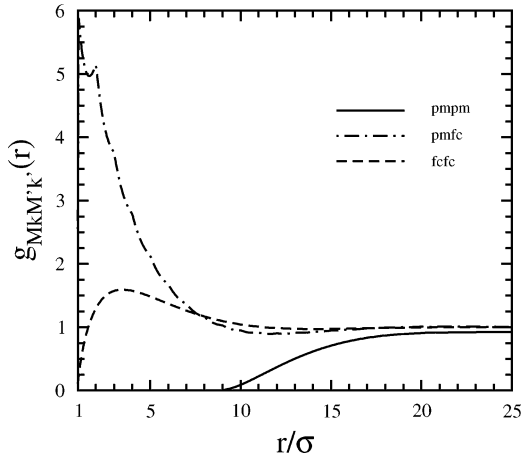

Figure 2. RO-RPA primitive model predictions for the partial radial-distribution functions $g_{MkM'k'}(r)$ as a function of scaled distance r/σ. The conditions are the same as in Figure 1.

$\sigma^{\text{eff}}_{pmpm}$ scales roughly as $\rho_m^{-1/2}$ in the semidilute regime, i.e., in a similar manner as the screening length ξ. On the other hand, as a function of charge density, $\sigma^{\text{eff}}_{pmpm}$ increases with increasing f, which is *opposite* to the behavior of ξ. This lack of complete correspondence should be kept in mind when interpreting the physical meaning of $\sigma^{\text{eff}}_{MkM'k'}$.

However, the RO prescription needs to be augmented for the two-state explicit model. For that model, as stated above, CC's are added to the chain such that it becomes a quasi-polyampholyte. If the CC's are a minority component, i.e., $N_{pc} \ll N_{pm}$, then upon range optimization, one also finds a moderate correlation hole for the pmpc and pcpc correlations but also a large enrichment near contact with a value equal to or greater than $g_{pmfc}(r)$. Since $\sigma^{\text{eff}}_{pmpm} \approx 9\sigma$ and the condensed counterions lie on the polymer backbone, the closest distance of approach of two CC's on different chains should be 7σ. Hence, this strong enrichment near contact seen in $g_{pmpc}(r)$ and $g_{pcpc}(r)$ is incorrect. Examination of other properties of the RPA theory seem to show that this incorrect behavior is an artifact of the RPA theory for heterogeneous polymers, though the effect is magnified by the range optimization scheme.

Both RO-RPA and PRISM theory employ an optimization scheme to handle strongly repulsive potentials

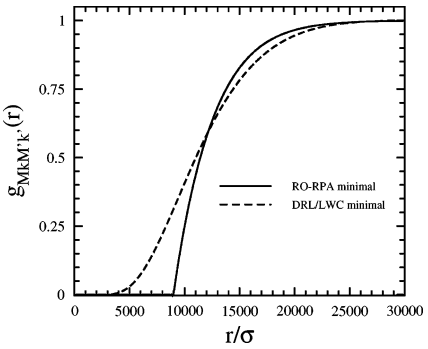

Figure 3. RO-RPA and DRL/LWC minimal model predictions for the monomer−monomer radial-distribution function $g_{mm}(r)$ as a function of scaled distance r/σ for $Z_m = 1$, $N_{pm} = 100$, and $\rho_m\sigma^3 = 10^{-11} \approx 0$. The DRL/LWC result is essentially exact at this density.

and it is well known that PRISM can yield an incorrect scaling for the critical temperature with molecular weight for polymer blends if the MSA closure is used.[47] On the other hand, the theory of CSL[45] has been shown to perform properly[44] with the MSA. The relevant difference between the two theories is thought to be that RISM-MSA is not diagrammatically proper while CSL-MSA is.[44,45] It is unclear at present whether the magnification of the anomalous behavior of the RPA seen here is related to deficiencies of PRISM-MSA. However, since the range optimization scheme is primarily a modification of the range of the hard-core potential within the MSA, its application to CSL theory would still allow CSL to remain diagrammatically proper. This application is thus worth exploring.

For the work here, a remedy to this defect can be easily accomplished for the chain model considered here. What we have done is just set $\sigma^{\text{eff}}_{pmpc}$ and $\sigma^{\text{eff}}_{pcpc}$ to have the smallest values consistent with the value of $\sigma^{\text{eff}}_{pmpm}$ and the positions of the CC's around the chain backbone. That is, we let $\sigma^{\text{eff}}_{pmpc} = \sigma^{\text{eff}}_{pmpm} - \sigma$ and $\sigma^{\text{eff}}_{pcpc} = \sigma^{\text{eff}}_{pmpm} - 2\sigma$, subject to the constraint that all $\sigma^{\text{eff}} \geq \sigma$. All results shown below for RO-RPA in the two-state explicit model employ this additional prescription.

In Figure 3, is shown the polymer monomer−monomer radial distribution function $g_{mm}(r)$ at $\rho_m\sigma^3 = 10^{-11}$, as predicted by the RO-RPA theory in the minimal model. The chains are fully charged, $Z_m = 1$, and the chain length $N_{pm} = 100$. Also shown are the predictions of the Laria−Wu−Chandler (LWC)[53] and Donley−Rajasekaran−Liu (DRL)[21] theories in the minimal model. For this chain length, $\rho^*\sigma^3 \approx 10^{-4}$, so this density is effectively zero. At this interaction energy, the correlation hole is much larger than the size of the polymer, so the polymer can be modeled as a point charge for polymer−polymer correlations. In this limit, the DRL and LWC theories are the same and essentially exact for $g_{mm}(r)$. It is well known that the RPA, while it predicts correctly the dependence of q_{max} with density in the dilute regime, $q_{max} \approx \rho_m^{1/3}$, also predicts a very negative $g_{mm}(r)$ within the correlation hole range. However, as can be seen, the RO-RPA yields a nonnegative $g_{mm}(r)$ as expected. Defining the correlation hole size, ξ_{ch}, as the distance at which $g_{mm}(r)$ reaches 1/2, one sees that the RO-RPA value for ξ_{ch} is within a few percent of the exact value. The RO-RPA then captures the essential characteristics of $g_{mm}(r)$ fairly accurately at these extremely low densities.

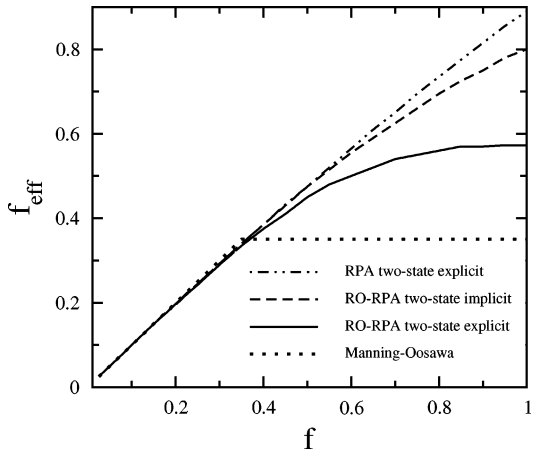

Figure 4. Effective chain charge fraction $f_{\text{eff}} \equiv f + Z_{\text{pc}}N_{\text{pc}}/N_{\text{pm}}$ as a function of chain charge fraction, f, for various theories and models. Here, $\rho_{\text{m}}\sigma^3 = 3 \times 10^{-3}$. The meaning of the curves is shown in the figure legend.

Since the radial distribution function is an isotropic average, it is not directly proportional to the counterion density distribution normal to a rod as computed by cell models using PB theory,[11,13] so a direct comparison between these quantities is not straightforward. However, since for polymer−counterion correlations RO-RPA yields approximately the same predictions as the RPA, it is not expected to perform as well as PB theory for these. On the other hand, as shown below, this lack of agreement may not matter much for polymer−polymer correlations.

3.2. Effective Chain Charge Fraction. The definition of a CC does not appear to be that clear for finite-density polyelectrolyte solutions as it is in the idealized M−O limit (zero density, infinite chain length).[5,6,15,28,29,54] As a consequence, quantities such as the number of CC's per chain are model dependent. Further, at nonzero concentrations, the number of "free" counterions, as defined by, e.g., conductivity measurements,[55] is not necessarily directly proportional to the fraction of noncondensed counterions. The former depends on the whole environment that a counterion is in, while the latter is just a measure of the departure of polymer−counterion correlations from whatever base theory is being used. Nevertheless, it is possible to examine effects within a particular model of condensation.

In Figure 4, is shown the effective charge fraction $f_{\text{eff}} \equiv f + N_{\text{pc}}/N_{\text{pm}}Z_{\text{pc}}$ as a function of chain charge fraction, f, at constant density $\rho_{\text{m}}\sigma^3 = 3 \times 10^{-3}$ within the two-state models for RPA and RO-RPA. The meanings of the curves are shown in the figure legend. As a reference, the dotted line gives the M−O[5,6] prediction. As mentioned above, while the computation of F_{tot} is essentially exact for the implicit model, it is approximate for the explicit model and tends to overestimate N_{pc}. We then regard the predictions for f_{eff} as underestimates for the explicit model (see the caveat below though). Given that, it is surprising how little condensation is predicted using the RPA theory. On the other hand, if one uses the RPA form for the free energy along with the RPA prediction for the $g(r)$'s, one obtains much more condensation than is obtained using the more-accurate eq 21. It is not uncommon in theory that an improvement of one aspect does not always improve the theory as a whole. It is interesting that one obtains much more condensation for RO-RPA in the explicit case than the implicit. In the explicit case, the CC's tend to order periodically and this structure has a lower energy than if they were all smeared out uniformly. It appears then that *intra*molecular correlations between CC's, neglected in the original M−O theory, become important for finite-density polyelectrolyte solutions.[56,57]

The effective charge fraction, f_{eff}, was also examined as a function of density, ρ_{m}, for fixed chain charge fraction $f = 1$. We find that f_{eff} decreases with decreasing density down to $\rho_{\text{m}} \approx \rho^*$, the overlap density, for both RPA and RO-RPA. Since $f_{\text{eff}} \to 1$ as $\rho_{\text{m}} \ll \rho^*$, f_{eff} appears to reach a minimum near ρ^*. For RPA, we find that $f_{\text{eff}} \approx 0.92$ for $\rho_{\text{m}}\sigma^3 = 0.03$ but drops to $f_{\text{eff}} \approx 0.63$ for $\rho_{\text{m}}\sigma^3 = 10^{-5} \approx \rho^*\sigma^3$. For RO-RPA, we find that $f_{\text{eff}} \approx 0.70$ for $\rho_{\text{m}}\sigma^3 = 0.03$ but drops to $f_{\text{eff}} \approx 0.43$ for $\rho_{\text{m}}\sigma^3 = 10^{-5} \approx \rho^*\sigma^3$. The predicted M−O threshold value for $f_{\text{eff}} = 0.35$ for our system, and so the RO-RPA result for f_{eff} near ρ^* is not far above that value. It is well known that the ordering in polyelectrolyte solutions (as determined by, e.g., the reduced viscosity) is strongest at densities near ρ^*, so it appears that the stronger the interactions become, the more condensation one obtains. Of course if $N_{\text{pm}} \to \infty$, then $\rho^* \to 0$, so one presumably recovers a result similar to that of M−O in that limit. However, since the original M−O theories model the CC's implicitly, it's possible that f_{eff} goes below the M−O threshold value in the explicit case.[56,57]

It is well known that D−H theory underestimates the strength of polymer−counterion correlations above the condensation threshold.[5] Since the density correlations for the CC's are determined by a simulation, it should provide then a better estimate of these correlations. It would seem then that a better estimate for the number of CC's could be obtained by allowing them to float freely in a cloud about the polymer backbone.[15] The cloud radius, ξ_{cl}, would then be determined by minimizing the free energy with respect to both it and N_{pc}. We have implemented this method for $\rho_{\text{m}}\sigma^3 = 0.003$. We find that for $f = 0.4$ and $f = 1.0$, $\xi_{\text{cl}} \approx 1.2\sigma$ and $\xi_{\text{cl}} > 8\sigma$, respectively. We find much more condensation at large f than the explicit CC model above predicts. Given the arguments above, these values for ξ_{cl} are reasonable. However, for this density, the largest value that ξ_{cl} can be is $(N_{\text{pm}}/(\pi L\rho_{\text{m}}))^{1/2} \approx 10\sigma$. Hence, at $f = 1.0$, the clouds are pretty much filling all space so all the counterions are condensed. On the other hand, since the RPA is being used as the base theory, these large clouds are a problem. The reason is that the RPA, like almost all approximate theories, assumes a sharp separation of energy scales that allows one to partition atoms into molecules. Monomers with relative positions that are approximately unchanged on the time scale of the measurement in which one is interested are considered as molecules in the RPA theory. Those that are not are considered as separate entities. Since the clouds are like-charged, they repel each strongly. This behavior is clearly unphysical since the counterions that are far from the polymer do not act collectively and can move freely past each other. One obtains then incorrect predictions for the liquid structure even though one is obtaining a better estimate for the free energy. The lesson here is not an uncommon one:[58] introducing elements into the theory to increase the accuracy of one quantity, such as the free energy, does not guarantee that the accuracy for any other quantity will not decrease, much less increase. At present, we are unable to determine any physical criterion that would set the value of ξ_{cl}. Given this, setting ξ_{cl} to its minimum

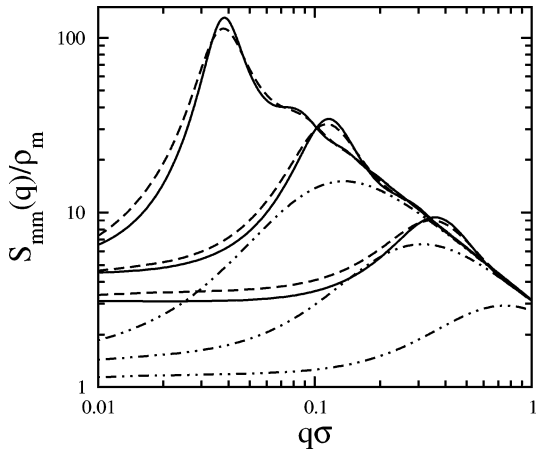

Figure 5. Scaled monomer−monomer structure factor $\hat{S}_{mm}(q)/\rho_m$ as a function of scaled wavevector $q\sigma$ for various theories and models at various densities. The chains are completely charged, so $Z_m \equiv f = 1$. The solid, dashed, and dot-dot-dashed lines correspond to results of the RO-RPA primitive, RO−RPA two-state explicit, and RPA two-state explicit models, respectively. For a given type of curve, the bottom, middle, and top curves correspond to densities $\rho_m\sigma^3 = 3 \times 10^{-3}$, 3×10^{-4}, and 3×10^{-5}, respectively.

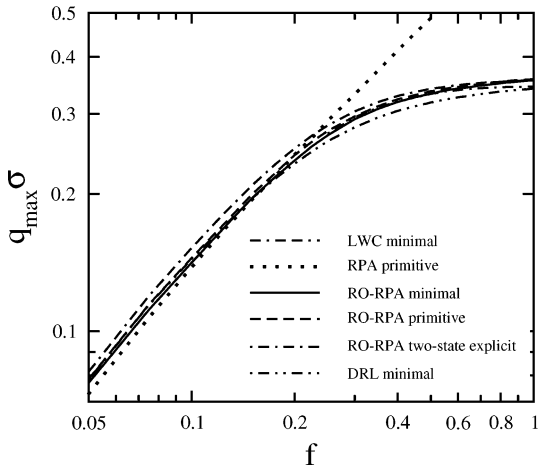

Figure 6. Scaled peak wavevector, $q_{max}\sigma$, of the monomer−monomer partial structure factor $\hat{S}_{mm}(q)$ as a function of the average fraction of charged monomers per chain f for $\rho_m\sigma^3 = 3 \times 10^{-3}$ for various theories and models. The meaning of the curves is shown in the figure legend.

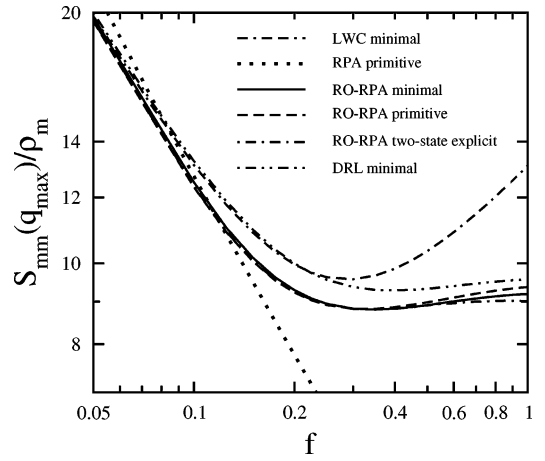

Figure 7. Scaled peak height of the monomer−monomer partial structure factor $\hat{S}_{mm}(q_{max})/\rho_m$ as a function of the average fraction of charged monomers per chain f for various theories and models. The conditions are the same as in Figure 6.

possible value of σ, as done in the two-state explicit model above, is most reasonable. We then regard the two-state explicit model as underestimating the amount of condensation at large f.

3.3. Structure Factor. Next, we examine results for more experimentally observable quantities such as the monomer−monomer structure factor and susceptibility. Figure 5 shows predicted values for the scaled monomer−monomer structure factor $\hat{S}_{mm}(q)/\rho_m$ as a function of scaled wavevector $q\sigma$ for the RO-RPA primitive and two-state explicit and RPA two-state explicit theories at various densities. The chains are fully charged, $Z_m \equiv f = 1$. In the semidilute regime, it is well known that q_{max} scales with monomer density as ρ_m^{ν}, with $\nu \approx 0.5$.[20,21,48,59,60] The RPA two-state yields $\nu \approx 0.37$. This value is slightly above the usual one for RPA for rods, 1/3. The probable reason for this difference is that, as the number of CC's increases with decreasing density, q_{max} decreases faster than it does without them. Both RO-RPA models give $\nu \approx 0.48-0.49$, which is consistent with the accepted value. So, it seems that the RO-RPA is modeling correctly the polymer−polymer correlation hole. The peak position, $\hat{S}_{mm}(q_{max})/\rho_m$, increases with decreasing density for all theories as expected.

Figures 6−8 show results for q_{max}, $\hat{S}_{mm}(q_{max})/\rho_m$, and $\hat{S}_{mm}(0)/\rho_m$, respectively, as a function of charge fraction, f, at constant density $\rho_m\sigma^3 = 3 \times 10^{-3}$ for various theories and models. At small f, q_{max}, $\hat{S}_{mm}(q_{max})/\rho_m$, and $\hat{S}_{mm}(0)/\rho_m$ increase, decrease, and decrease, respectively, with increasing f with both RPA and RO-RPA being almost in quantitative agreement. Differences between the two theories at small f are due to RO-RPA capturing the hard-core behavior of the chains at the level of PRISM theory. On the other hand, at large $f \geq 0.4$, it is clear that range optimization completely changes the character of the RO-RPA theory. In contrast to the RPA, RO-RPA in the minimal model predicts that all these quantities become pretty much constant. This invariance of q_{max} and $\hat{S}_{mm}(q_{max})/\rho_m$ is in qualitative agreement with experiments on flexible polyelectrolytes of Nishida, Kaji, and Kanaya (NKK)[26] and Essafi, Lafuma, and Williams (ELW).[27] Note that adding explicit counterions via the primitive model and condensed counterions via the two-state models produce only moderate change in the theoretical trends for all three quantities.

To help determine the validity of the RO-RPA theory, we also show results for two other theories: LWC[53] and DRL.[21] The reference version of LWC[62] has been applied to polyelectrolyte solutions by Shew and Yethiraj[20,23] and others.[25] Both DRL and LWC are approximations to the "two-chain" equation[53,63] for the radial distribution function. The main difference between them is that DRL includes more monomer-level correlations that allow the theory to handle hard-core interactions and possibly better describe molecules with oppositely charged sites. Laria, Wu, and Chandler have discussed the consequences of their approximation for this latter system.[53] In the primitive model, we were able to find convergent solutions for both LWC and DRL up to $f \approx 0.5$ for the case considered here. Whether a solution exists for these theories for this model at higher charge densities is an open question.[21,25] On the other hand, there appears to be no such problem for these theories within the minimal model. Thus, since we find no significant differences between the models for $\hat{S}_{mm}(q)$ for the case here, only results for the minimal will be

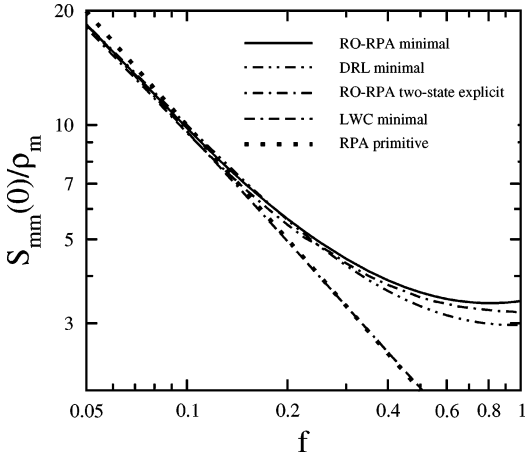

Figure 8. Scaled susceptibility of the monomer−monomer partial structure factor $\hat{S}_{mm}(0)/\rho_m$ as a function of the average fraction of charged monomers per chain f. The conditions are the same as in Figure 6. The effectively straight lines are the RPA and LWC predictions, which overlap.

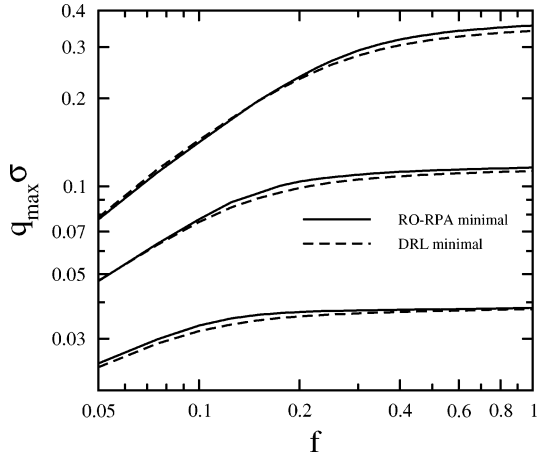

Figure 9. Scaled peak wavevector, $q_{max}\sigma$, of the monomer−monomer partial structure factor $\hat{S}_{mm}(q)$ as a function of the average fraction of charged monomers per chain f for various densities and theories. The meaning of the type of curves is shown in the figure legend. For a given type of line, the top, middle, and bottom curves correspond to densities $\rho_m\sigma^3 = 3 \times 10^{-3}$, 3×10^{-4}, and 3×10^{-5}, respectively.

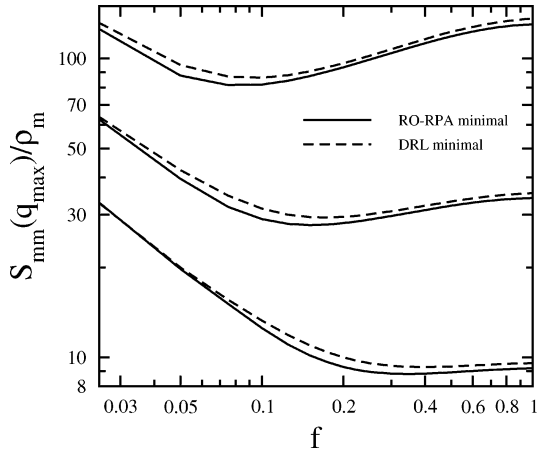

Figure 10. Scaled peak height of the monomer−monomer partial structure factor $\hat{S}_{mm}(q_{max})/\rho_m$ as a function of the average fraction of charged monomers per chain f for various densities and theories. For a given type of line, the bottom, middle, and top curves correspond to densities $\rho_m\sigma^3 = 3 \times 10^{-3}$, 3×10^{-4}, and 3×10^{-5}, respectively.

shown. As can be seen, the DRL[64] theory also produces an invariance at large f and agrees almost quantitatively with RO-RPA at all values of f. Such agreement is notable because the DRL theory can be regarded as more sophisticated than RO-RPA. DRL builds in the proper low-density behavior in the atomic case (as LWC does) and includes molecular- and monomer-level correlations not present in the RPA theory.[21] Range optimization seems to incorporate these correlations well enough to yield effectively the same result, but in a simpler manner. LWC also agrees with RO-RPA for q_{max}, but not for $\hat{S}_{mm}(q)/\rho_m$ and $\hat{S}_{mm}(0)/\rho_m$ at large f. Indeed, the predictions of LWC for $\hat{S}_{mm}(0)/\rho_m$ are essentially identical to those of the RPA. In the absence of any hard comparison with simulation or experiment, the proper behavior at large f is unknown. However, given the close agreement of RO-RPA and DRL and given that DRL can be regarded as an improvement on LWC, we regard the predictions of RO-RPA to be more realistic.

It can be argued that since the D−H screening length $\xi \approx 3\sigma$ at the highest charge fraction for this density, all counterions are so close to the chain that they act as condensed ones. Hence, at lower densities where ξ is much larger, this invariance may not hold for theories that model polymer−counterion correlations at the level of D−H theory. To explore this issue, we also examined the behavior of these quantities at much lower densities. Figures 9 and 10 show results for q_{max} and $\hat{S}_{mm}(q_{max})/\rho_m$, respectively, as a function of charge fraction, f, at various densities for various theories and models. The smallest density gives $\xi \approx 30\sigma$ at $f = 1$. As can be seen, q_{max} becomes even more invariant at lower densities with the onset occurring at $f \approx 0.2$ for both theories at the lowest density. This onset value is *lower* than that obtained using a M−O counterion condensation argument, 0.35. Experiments of NKK[26] seem to show that the onset is approximately the same for all the densities they examined and agrees roughly with the M−O value; hence, it is possible that chain flexibility has some effect here. The invariance of $\hat{S}_{mm}(q_{max})/\rho_m$ at these lower densities is less than that for the highest one. The only quantitative experimental evidence for an invariance is due to ELW, and their data is for densities near the largest one covered here: $\rho_m\sigma^3 = 3 \times 10^{-3}$.[27] However, since the amount of condensation increases as $\rho_m \rightarrow \rho^*$, it is expected that the difference between the predictions of the minimal and two-state models to be greatest for $\hat{S}_{mm}(q_{max})/\rho_m$ near ρ^*. An explanation for this invariance with f seen by the theory is due to screening: as f increases, the repulsion between polymer chains increases; on the other hand, charge neutrality forces more and more counterions into the solution which increases the screening between polymers. At small f, polymer and counterion correlations are weak, but at large f, they increase such that one reaches a balance between polymer−polymer repulsion and counterion screening.

The RO-RPA in the primitive and two-state explicit models predict (not shown) that the susceptibility $\chi_T \equiv \hat{S}_{mm}(0)/\rho_m$ increases with decreasing density down to about $\rho_m\sigma^3 \approx 3 \times 10^{-5}$, reaches a maximum, and then decreases again with decreasing density. This maximum occurs at about $3\rho^*$. The RPA predicts that $\hat{S}_{mm}(0)/\rho_m$ increases with decreasing density down to the smallest density we examined, $\rho_m\sigma^3 = 10^{-6} = \rho^*\sigma^3/10$. Normally, this maximum in the susceptibility predicted by the RO-RPA would be associated with a maximum of CC's, but

the RO-RPA primitive gives basically D−H polymer−counterion correlations, i.e., it does not contain any CC's. So, presumably the maximum in $\hat{S}_{mm}(0)/\rho_m$ is due to polymer−polymer correlations. The susceptibility is equal to $1/\rho_m(\partial\rho_m/\partial\mu_m)_{V,T} = (\partial\Pi/\partial\rho_m)_{V,T}^{-1}$, where μ_m is the monomer chemical potential and Π is the osmotic pressure. This latter derivative is then also a maximum near ρ^*.

The results above for the susceptibility prompt two questions: 1) Since the structure route is being used, how realistic are these predictions within the minimal or primitive models? 2) How are the predictions of these models for the susceptibility relevant to real polyelectrolyte solutions? Consider question 1 first. Almost all theories of charged systems predict no divergence of the structure factor near an apparent critical point.[65] This thermodynamic inconsistency also holds for the present theory (at least within the minimal and primitive models). The difference between the free energy and structure routes for computing thermodynamic quantities is one of cause versus mechanism. The free energy route merely compares the energy of two possible states; the structure route gives an indication of *how* the phase separation occurs. Since it is known that charged liquids can phase-separate from the solvent under certain conditions and the free energy route has been shown to predict this,[30,66] it appears then that that route should be used preferably to compute any thermodynamic quantity. Hence, the above predictions for the susceptibility from the structure route, while probably correct within the minimal model, should be interpreted with caution for models with explicit counterions. On the other hand, as shown in the next section, the theory above can also be used to compute the osmotic pressure from the free energy route. We find that $(\partial\Pi/\partial\rho_m)_{V,T}^{-1} \approx 6$ for $f = 1$ at the above density for the two-state explicit model. This value is not that far above that predicted by the structure route. Now, consider question 2. It is unclear at present what is the behavior of the susceptibility of a "model" polyelectrolyte solution. There are many scattering experiments that show very large low-wavevector scattering, i.e., a "slow mode".[2−4,61] On the other hand, of the experiments that measure the density dependence of the osmotic pressure[2,11] we know of none that show any anomalously small variation of Π with density ρ_m that would indicate the same effect. There have been arguments that if the "slow mode" phenomenon is indeed intrinsic to polyelectrolyte solutions, it is due to ingredients not contained within the primitive (or minimal) model of polyelectrolytes.[2] Our results here do not contradict these arguments.

3.4. Osmotic Pressure. While this theory is primarily one for liquid structure, it is interesting to examine its predictions for the osmotic pressure. Since the system contains only an implicit solvent, the osmotic pressure $\Pi = (\partial F_{tot}/\partial V)_{T,N_p}$, where F_{tot} is given by eq 20 above. As we've already computed F_{tot} to determine N_{pc}, this derivative is determined using finite differences. The osmotic pressure of polyelectrolyte solutions has been examined intensely by experiment, simulation, and theory;[2,9,11] however, there is one interesting aspect that we believe the RO-RPA theory can illuminate.

In Figure 11, the scaled pressure, Π/ρ_m, is plotted as a function of the charge fraction, f, for fixed density $\rho_m\sigma^3 = 3 \times 10^{-3}$ for various theories and models. The quantity Π/ρ_m equals the osmotic coefficient ϕ at $f = 1$ since $\rho_m = \rho_c$ there. At small f, the pressure increases

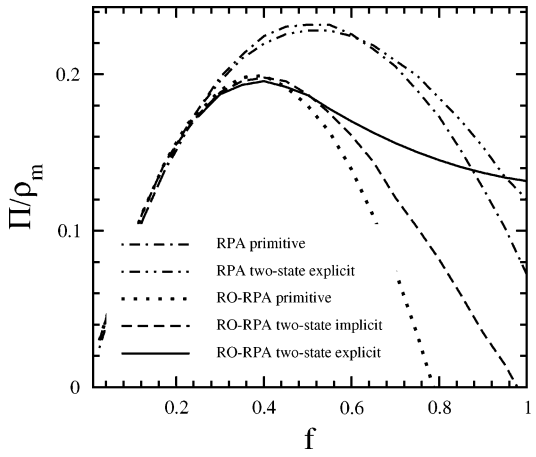

Figure 11. Scaled osmotic pressure Π/ρ_m (equals the osmotic coefficient at $f = 1$ since $\rho_m = \rho_c$ there) as a function of per chain charge fraction f for density $\rho_m\sigma^3 = 3 \times 10^{-3}$ for various theories and models. The break in the dotted curve is due to the overlap of the figure legend.

with increasing f for all theories and models. At $f \approx 0.4$ and 0.5 for the RO-RPA and RPA theories, respectively, the pressure reaches a maximum and then starts to decrease with increasing f. The RPA primitive predicts that $\Pi/\rho_m \approx 0.075$ at $f = 1$ which also is its value at $f = 0.1$. Adding CC's increases this value somewhat to 0.125 at $f = 1$.[67] On the other hand, RO-RPA primitive predicts that the pressure becomes *negative* at large f, implying that the system becomes unstable to macrophase separation. Since there appears to be no evidence that model polyelectrolytes with monovalent counterions phase separate at these Bjerrum lengths,[11,14] what is the reason for this behavior?

A probable one is due to the asymmetry of range optimization: it improves correlations between repulsive monomers but yields less improvement for attractive ones. It would seem then that improving polymer−counterion correlations by adding condensed counterions would remedy matters. As can be seen, adding CC's with the two-state implicit model helps to stabilize the system somewhat, but Π is still negative at $f = 1$. However, adding CC's with the two-state explicit model stabilizes the solution. Indeed, the explicit model gives a value of $\Pi/\rho_m \approx 0.13$ at $f = 1$, which is not deeply far below its peak value of 0.19. It is interesting that Π/ρ_m is a maximum at a charge fraction just above the M−O counterion condensation onset value $f^* = 0.35$. Recent experiments on flexible polyelectrolytes have shown that the osmotic pressure as a function of f can become pretty much constant above this threshold.[68] Our results are only in partial agreement with that, though if we had set the cloud radius $\xi_{cl} = 2\sigma$, Π would have been constant for $f > 0.4$. Hence, the uncertainty in ξ_{cl} and differences in chain structure[28] are two possible reasons for this lack of agreement. It is expected that the osmotic pressure becomes insensitive to the degree of accuracy of the CC model once that model has reached a certain level of realism. From the above results, it appears that the two-state explicit model is close but more work needs to be done.

This stabilization by counterions (or just charges) is a common property of many complex fluids.[4,8,69,70] It is interesting that, on one hand, a local, microphase separation of the counterions with single chains stabilizes the fluid, but at lower temperatures, even this energy drop can be insufficient such that the polymers

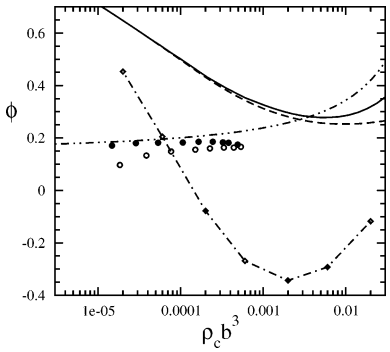

Figure 12. Osmotic coefficient, $\phi \equiv \Pi/\rho_c$, as a function of scaled counterion density $\rho_c b^3$. The solid and open circles correspond to experimental data on PPP-1 of Blaul et al. for chlorine and iodine counterions, respectively. The solid, dashed, and dot-dashed (with diamonds) lines correspond to predictions of the RO-RPA theory within the primitive model by the structure route, minimal model by the structure route, and primitive model by the free energy route, respectively. The dot-dot-dashed line is the prediction of Poisson−Boltzmann theory within the cell model.

and counterions eventually macrophase-separate from the solvent.

Last, we show results for the osmotic coefficient, $\phi \equiv \Pi/\rho_c$, as a function of density. We compare the predictions of the present theory with recent experiments of Blaul, Wittemann, Ballauff, and Rehahn using a fully charged rodlike polymer with a poly-*p*-phenylene backbone, denoted as PPP-1.[11,71,72] For their system, $l_B = 7.3$ Å, $b = 4.3$ Å, $N_{pm} \approx 40$, $Z_m = 2$, $Z_c = -1$, $\sigma_{mc} \approx 7$ Å, and $\sigma_{cc} \approx 4.4$ Å. Presumably then, $\sigma_{mm} \approx 9.6$ Å. Since we are using the primitive model in which all hard-core diameters are the same, we let $\sigma_{ij} = b$ for all i and j. The interaction energy of this system is larger than the one considered above, so that, from a Manning argument, we can expect that $N_{pc}/N_{pm} \approx 1.4$. As mentioned above, the accuracy of our model of CC's is limited to $N_{pc}/N_{pm} \leq 1/2$; hence, it is not expected to be that quantitatively accurate here. We have performed some rough calculations that show that RO-RPA within the two-state explicit model will give a value for ϕ somewhere between 0.13 and 0.2 for semidilute densities (ignoring very high densities). However, any further increase in accuracy requires an improvement in this CC model. Hence, we do not show results of the two-state explicit model here. However, we do show results for the primitive model for both the structure and free energy routes. Both these results are incorrect given our arguments above, but they do show some interesting aspects of our theory and the rod polyelectrolyte system itself.

In Figure 12, is shown the osmotic coefficient, ϕ, as a function of scaled counterion density $\rho_c b^3$ for the RO-RPA in the primitive model computed from the structure and free energy routes and in the minimal model from the structure route. Also shown are data of Blaul et al. using chlorine and iodine (monovalent) counterions[71] and the predictions of Poisson−Boltzmann theory in the cell model.[7,72] Surprisingly, the structure route results for RO-RPA show a large decrease in the osmotic pressure in the semidilute regime ($\rho_m^* b^3 \approx 10^{-3}$ for this system) so that the minimum of $\phi \approx 0.25-0.27$ which is only about 35% above the experimental values for the chlorine ion data. It appears then that polymer−polymer correlations are mimicking the effects of counterion condensation in a similar manner as they do for $\hat{S}_{mm}(q)$ mentioned in Section 3.3 above. On the other hand, ϕ by the free energy route is very negative for densities in or near the semidilute regime. At large densities, there should be a transition to a nematic phase for rods. However, as for the case shown in Figure 11 above, including explicit condensed counterions is expected to stabilize the system before this transition is reached. In this figure, the agreement between PB theory and experiment appears to be very good, as is the agreement between PB theory and molecular dynamics simulations of the cell model on the same system (data not shown) in the same dilute density range as that covered by the experimental data.[72]

4. Summary and Conclusions

In conclusion, we have presented a new optimization scheme that improves substantially the predictive power of the RPA theory for the structure of polyelectrolyte solutions. For example, it enables the RPA to predict well the zero density form of the monomer−monomer radial distribution function and yield the accepted scaling exponent of q_{max} with density, 1/2. As applied to the RPA, this scheme can be regarded as one way to extend polymer−RISM theory to charged molecules.

We showed that this range-optimized RPA in the minimal model predicts an invariance in the peak position and peak height of the structure factor at high charge fraction, f, in qualitative agreement with recent experimental data of Essafi, Lafuma, and Willaims.[27] We find that this invariance is strongest for q_{max} at lower densities near ρ^* and is strongest for $S_{mm}(q_{max})$ at higher densities (excluding melt-like densities). We also showed that another theory, DRL, gave very similar results adding weight to the conclusion that this predicted behavior is indeed correct within the minimal model. We thus find that it is not necessary to invoke more complex mechanisms, such as counterion condensation, to explain these effects. It appears then that this invariance may be a more general property of such systems than any particular physical mechanism that can cause it. On the other hand, for the osmotic pressure, we find that CC's are a necessary element in (or at least one means of) stabilizing the liquid against macrophase separation—but one must go beyond the M−O theory and include *intra*chain correlations between CC's to produce this physical behavior. For thermodynamics, it then seems to be important to balance improvements in correlations between like-charged monomers (as done by the range-optimization scheme) with those for oppositely charged monomers (as done by including condensed counterions). It is interesting then to note the contrast between the ingredients needed to produce signature behavior for the liquid structure and those for the liquid thermodynamics.

In Section 3.3, we noted that there is an inconsistency between experiments that show an anomalously large scattering intensity at low wavevectors and those that measure the osmotic coefficient. Our theory here gives values for the susceptibility from both the structure and free energy routes that are only comparable to the scaled peak value, $\hat{S}_{mm}(q_{max})/\rho_m$, not orders of magnitude larger. This result could be expected since effects such as "counterion-induced attractions" are not modeled well here since the base theory is RPA. However, the theory's predictions for the osmotic pressure when the two-state explicit model is used are comparable with those obtained from experiment and Poisson−Boltzmann

theory. It seems then that the origin of this large low-wavevector scattering, aka, "slow mode", may be other than a large polyelectrolyte susceptibility. To help clarify this situation, it would be very useful to have a set of experiments on the same system that compute $(\partial\Pi/\partial\rho_m)_{V,T}$ by different methods, including light scattering, to determine if a consistent measurement is obtained if a slow mode is present.

Improvements in our chain model are necessary to make detailed comparisons with simulations or experiments of flexible polyelectrolytes. The range-optimization procedure as applied to the RPA may be adequate for this task, but it is general enough to be employed in other theories if necessary. As discussed in Section 2.1, it can be applied to any approximate theory that violates the positivity requirement on the radial distribution functions. It is possibly of use then to applications of the CSL[43−45] (see also the discussion in Section 3.1 above), Wertheim,[38,73−75] and other generalizations of OZ theory to polyelectrolytes. Since this positivity requirement on $g(r)$ can also be violated at low temperatures for electrolytes, this technique may also find use in OZ-MSA theory.

Acknowledgment. We thank John G. Curro and Craig E. Pryor for helpful conversations and correspondence and Theodore Kim for help with our computing facilities. Sandia is a multiprogram laboratory operated by Sandia Corporation, a Lockheed Martin Company, for the United States Department of Energy's National Nuclear Security Administration under Contract No. DE-AC04-94AL85000.

References and Notes

(1) An abridged description of the theory is given in: Donley, J. P.; Heine, D. R.; Wu, D. T. www.arxiv.org/cond-mat/0305449.
(2) Hara, M. *Polyelectrolytes: Science and Technology*; Marcel-Dekker: New York, 1993. Förster, S.; Schmidt, M. *Adv. Polym. Sci*. **1995**, *120*, 52.
(3) Williams, C. E. In *Electrostatic Effects in Soft Matter and Biophysics*, *NATO Science Series II: Mathematics, Physics and Chemistry*; Holm, C., Kekicheff, P., Podgornik, R., Eds.; Kluwer Academic: Dordrecht, 2001; Vol 46.
(4) *Physical Chemistry of Polyelectrolytes, Surfactant Science Series*; Radeva, T., Ed.; Marcel Dekker: New York, 2001; Vol. 99.
(5) Manning, G. S. *J. Chem. Phys.* **1969**, *51*, 924.
(6) Oosawa, F. *Polyelectrolytes*; Marcel Dekker: New York, 1971.
(7) Fuoss, R. M.; Katchalsky, A.; Lifson, S. *Proc. Natl. Acad. Sci. U.S.A.* **1951**, *37*, 579. Alfrey, T.; Berg, T. W.; Morawetz, H. *J. Polym. Sci*. **1951**, *7*, 543.
(8) Katchalsky, A. *Pure Appl. Chem.* **1971**, *26*, 327.
(9) Das, T.; Bratko, D.; Bhuiyan, L. B.; Outhwaite, C. W. *J. Phys. Chem.* **1995**, *99*, 410. Ibid. *J. Chem. Phys.* **1997**, *107*, 9197.
(10) Deserno, M.; Holm, C.; Blaul, J.; Ballauff, M.; Rehahn, M. *Eur. Phys. J. E* **2000**, *5*, 97. Deserno, M.; Holm, C.; May, S. *Macromolecules* **2000**, *33*, 199.
(11) Holm, C.; Rehahn, M.; Oppermann, W.; Ballauff, M. *Adv. Polym. Sci*. **2004**, *166*, 1, and references therein.
(12) Borukhov, I.; Andelman, D.; Orland, H. *Phys. Rev. Lett.* **1997**, *79*, 435. Borukhov, I.; Andelman, D.; Orland, H. *Electrochim. Acta* **2000**, *46*, 221.
(13) Deshkovski, A.; Obukhov, S.; Rubinstein, M. *Phys. Rev. Lett*. **2001**, *86*, 2341.
(14) Liao, Q.; Dobrynin, A. V.; Rubinstein, M. *Macromolecules* **2003**, *36*, 3399.
(15) Ray, J.; Manning, G. S. *Langmuir* **1994**, *10*, 2450. Ibid. *Macromolecules* **2000**, *33*, 2901.
(16) Barrat, J.-L.; Joanny, J.-F. *Adv. Chem. Phys.* **1996**, *54*, 1.
(17) Ha, B.-Y.; Liu, A. J. *Phys. Rev. Lett*. **1997**, *79*, 1289.
(18) Nilsson, L. G.; Guldbrand, L.; Nordensklöld, L. *Mol. Phys*. **1991**, *72*, 177.
(19) Muthukumar, M.; Edwards, S. F. *J. Chem. Phys*. **1982**, *76*, 2720. Muthukumar, M. *J. Chem. Phys.* **1996**, *105*, 5183.
(20) Yethiraj, A.; Shew, C.-Y. *Phys. Rev. Lett*. **1996**, *77*, 3937. Shew, C.-Y.; Yethiraj, A. *J. Chem. Phys.* **1997**, *106*, 5706.
(21) Donley, J. P.; Rajasekaran, J. J.; Liu, A. J. *J. Chem. Phys.* **1998**, *109*, 849. Donley, J. P. *J. Chem. Phys.* **2002**, *116*, 5315. Donley, J. P. *J. Chem. Phys.* **2004**, *120*, 1661.
(22) Canessa, E.; D'Aguanno, B.; Weyerich, B.; Klein, R. *Mol. Phys.* **1991**, *73*, 175.
(23) Shew, C.-Y.; Yethiraj, A. *J. Chem. Phys.* **1999**, *110*, 11599.
(24) Dymitrowska, M.; Belloni, L. *J. Chem. Phys.* **1999**, *111*, 6633.
(25) Hofmann, T.; Winkler, R. G.; Reineker, P. *J. Chem. Phys.* **2001**, *114*, 10181.
(26) Nishida, K.; Kaji, K.; Kanaya, T. *Macromolecules* **1995**, *28*, 2472.
(27) Essafi, W.; Lafuma, F.; Williams, C. E. *Eur. Phys. J. B* **1999**, *9*, 261.
(28) Gonzalez-Mozuelos, P.; Olvera de la Cruz, M. *J. Chem. Phys.* **1995**, *103*, 3145. Olvera de la Cruz, M.; Belloni, L.; Delsanti, M.; Dalbiez, J. P.; Spalla, O.; Drifford, M. *J. Chem. Phys.* **1995**, *103*, 5781.
(29) Nyquist, R. M.; Ha, B.-Y.; Liu, A. J. *Macromolecules* **1999**, *32*, 3481.
(30) Ermoshkin, A. V.; Olvera de la Cruz, M. *Macromolecules* **2003**, *36*, 7824.
(31) Fisher, M. E.; Levin, Y. *Phys. Rev. Lett*. **1993**, *71*, 3826, and references therein.
(32) Pickett, G. T.; Schweizer, K. S. *J. Chem. Phys.* **2000**, *112*, 4881.
(33) Chandler, D.; Singh, Y.; Richardson, D. M. *J. Chem. Phys.* **1984**, *81*, 1975.
(34) Melenkevitz, J.; Schweizer, K. S.; Curro, J. G. *Macromolecules* **1993**, *26*, 6190.
(35) Donley, J. P.; Rudnick, J.; Liu, A. J. *Macromolecules* **1997**, *30*, 1188.
(36) Negele, J. W.; Orland, H. *Quantum Many-Particle Systems*; Westview Press: Boulder, CO, 1998.
(37) Fredrickson, G. H.; Ganesan, V.; Drolet, F. *Macromolecules* **2002**, *35*, 16.
(38) Jiang, J. W.; Blum, L.; Bernard, O.; Prausnitz, J. M. *Mol. Phys.* **2001**, *99*, 1121.
(39) Andersen, H. C.; Chandler, D. *J. Chem. Phys.* **1972**, *57*, 1918.
(40) Andersen, H. C.; Chandler, D. *J. Chem. Phys.* **1971**, *55*, 1497.
(41) Lebowitz, J. L.; Percus, J. K. *Phys. Rev*. **1966**, *144*, 251.
(42) Ornstein, L. S.; Zernike, F. *Proc. Acad. Sci. Amsterdam* **1914**, *17*, 793.
(43) Lupkowski, M.; Monson, P. A. *J. Chem. Phys.* **1987**, *87*, 3618. Lupkowski, M.; Monson, P. A. *Mol. Phys*. **1988**, *63*, 875. McGuigan, D. B.; Lupkowski, M.; Paquet, D. M.; Monson, P. A. *Mol. Phys.* **1989**, *67*, 33.
(44) Melenkevitz, J.; Curro, J. G. *J. Chem. Phys.* **1996**, *106*, 1216. Ibid. **1997**, *106*, 8221.
(45) Chandler, D.; Silbey, R.; Ladanyi, B. M. *Mol. Phys.* **1982**, *46*, 1335.
(46) Chandler, D.; Andersen, H. C. *J. Chem. Phys.* **1972**, *57*, 1930. Chandler, D. *Phys. Rev. E* **1993**, *48*, 2898.
(47) Schweizer, K. S.; Curro, J. G. *Phys. Rev. Lett* **1987**, *58*, 246. Curro, J. G.; Schweizer, K. S. *Macromolecules* **1987**, *20*, 1928. Schweizer, K. S.; Curro, J. G. *Adv. Chem. Phys*. **1997**, *98*, 1.
(48) de Gennes, P. G.; Pincus, P.; Velasco, R. M.; Brochard, F. *J. Phys. (Paris)* **1976**, *37*, 1461.
(49) Hansen, J. P.; McDonald, I. R. *Theory of Simple Liquids*; Academic Press: London, 1986.
(50) Hoye, J. S.; Lomba, E.; Stell, G. *Mol. Phys.* **1992**, *75*, 1217.
(51) Edwards, S. F. *Proc. Phys. Soc. London* **1965**, *85*, 613.
(52) Chandler, D. In *Studies in Statistical Mechanics*; Montroll, E. W., Lebowitz, J. L., Eds.; North-Holland: Amsterdam, 1982; Vol. 8.
(53) Laria, D.; Wu, D.; Chandler, D. *J. Chem. Phys.* **1991**, *95*, 4444.
(54) Levin, Y.; Barbosa, M. C. *J. Phys. II France* **1997**, *7*, 37.
(55) Bordi, F.; Colby, R. H.; Canetti, C.; De Lorenzo, L.; Gili, T. *J. Phys. Chem. B* **2002**, *106*, 6887, and references therein.
(56) Fenley, M. O.; Manning, G. S.; Olson, W. K. *Biopolymers* **1990**, *30*, 1191.
(57) Henle, M. L.; Santangelo, C. D.; Patel, D. M.; Pincus, P. A. *APS Bulletin* **2004**.
(58) Doi, M.; Edwards, S. F., *The Theory of Polymer Dynamics*; Clarendon Press: Oxford, 1986.
(59) Maier, E. E.; Krause, R.; Deggelmann, M.; Hagenbüchle, M.; Weber, R.; Fraden, S. *Macromolecules* **1992**, *25*, 1125. Guilleaume, B.; Blaul, J.; Ballauff, M.; Wittemann, M.; Rehahn, M.; Goerigk, G. *Eur. Phys. J. E* **2002**, *8*, 299.
(60) Stevens, M. J.; Kremer, K. *J. Chem. Phys.* **1995**, *103*, 1669.
(61) Ermi, B. D.; Amis, E. J. *Macromolecules* **1998**, *31*, 7378, and references therein.

(62) Schweizer, K. S.; Yethiraj, A. *J. Chem. Phys.* **1993**, *98*, 9053.
(63) Donley, J. P.; Curro, J. G.; McCoy, J. D. *J. Chem. Phys.* **1994**, *101*, 3205.
(64) The exponent η that appears in the DRL theory has been set to 1/2 for the results shown here.
(65) A divergent susceptibility can be obtained possibly from the structure route for an electrolyte liquid if the two-state model is employed. See: Lee, B. P.; Fisher, M. E. *Phys. Rev. Lett* **1996**, *76*, 2906.
(66) Friedman, H. L.; Larsen, B. *J. Chem. Phys.* **1979**, *70*, 92, and references therein.
(67) This non-monotonic behavior is contrary to predictions of the RPA when the RPA form of the free energy is used to compute Π.[28,29] It can be argued that RPA predictions for the $g_{MkM'k'}(r)$'s have meaning only within the RPA form for the free energy since the level of approximation is the same for both. This argument should be kept in mind when interpreting our predictions of the RPA for Π.
(68) Williams, C. E.; Essafi, W.; Baigl, D. *APS Bulletin* **2004**.
(69) Khokhlov, A. R.; Nyrkova, I. A. *Macromolecules* **1992**, *25*, 1493, and references therein.
(70) Nomula, S.; Cooper, S. L. *J. Phys. Chem. B* **2000**, *104*, 6963.
(71) Blaul, J.; Wittemann, M.; Ballauff, M.; Rehahn, M. *J. Phys. Chem. B* **2000**, *104*, 7077.
(72) Deserno, M.; Holm, C.; Blaul, J.; Ballauff, M.; Rehahn, M. *Eur. Phys. J. E* **2001**, *5*, 97.
(73) Wertheim, M. S. *J. Stat. Phys*. **1984**, *35*, 19. Ibid. **1984**, *35*, 35. Ibid. **1986**, *42*, 459. Ibid. **1986**, *42*, 477.
(74) von Solms, N.; Chiew, Y. C. *J. Chem. Phys.* **1999**, *111*, 4839. Ibid. **2003**, *118*, 4321.
(75) Bernard, O.; Blum, L. *J. Chem. Phys.* **2000**, *112*, 7227.

MA049264M